



Cite this: *Sustainable Energy Fuels*, 2021, 5, 1085

## Demonstration of green hydrogen production using solar energy at 28% efficiency and evaluation of its economic viability†

M. A. Khan, I. Al-Shankiti, A. Ziani and H. Idriss \*

The solar to hydrogen (STH) efficiency of photovoltaic-electrolysis (PV-E) setups is a key parameter to lower the cost of green hydrogen produced. Commercial c-Si solar cells have neared saturation with respect to their efficiency, which warrants the need to look at alternative technologies. In this work, we report a concentrator photovoltaic-electrolysis (CPV-E) setup with a STH efficiency of 28% at 41 suns (without the use of Fresnel lenses), the highest reported efficiency using an alkaline system to date. Using this as a base case, we carried out a detailed techno-economic (TEA) analysis, which showed that despite the high cost associated with CPV cells, the levelized cost of hydrogen (LCOH) is at  $\$5.9\text{ kg}^{-1}$ , close to that from c-Si solar farms ( $\$4.9\text{ kg}^{-1}$ ), primarily due to the high STH efficiency. We also report sensitivity analysis of factors affecting both CPV and alkaline electrolyser systems such as the CPV module efficiency and installed capacity, electrolyser stack lifetime, operating current density, and working hours. Our results indicate that in a scenario where the installed capacity of CPV technology matches that of silicon and with an electrolyser operating current density of  $\sim 0.7\text{ A cm}^{-2}$ , the LCOH from CPV-electrolysis systems can be  $<\$2\text{ kg}^{-1}$ . These results demonstrate the potential of CPV technology for large-scale green hydrogen production to replace that obtained from fossil fuels.

Received 30th November 2020  
Accepted 6th January 2021

DOI: 10.1039/d0se01761b  
[rsc.li/sustainable-energy](http://rsc.li/sustainable-energy)

## 1. Introduction

Molecular hydrogen as an energy vector helps in decarbonizing our energy system in order to achieve the emission reduction goals, for example as stated in the Paris Agreement. To make a meaningful difference and achieve net zero emissions, hydrogen will have to be produced *via* water splitting using renewable electricity. Solar photovoltaic (PV) power represents one of the cheapest and most widely deployed sources of renewable electricity with over 520 GW of cumulative installed capacity worldwide as of 2018.<sup>1,2</sup> For that reason, it is considered as the prime vector of energy to power green hydrogen production. While there are other methods of solar hydrogen production such as photocatalytic reactions<sup>3</sup> and direct photoelectrochemical water splitting,<sup>4,5</sup> present day technology is only available for decoupled PV-electrolysis (PV-E) systems. Silicon based PV cells dominate the market with  $\sim 95\%$  share of current production,<sup>1</sup> and have seen their cost dropping significantly in the last few years. Nonetheless, the estimated cost of green H<sub>2</sub> from silicon-based PV-E is still very high for sustainable production. It varies widely depending on the nature and

level of studies:  $\$3\text{--}17\text{ kg}^{-1}$ ,<sup>6</sup>  $\$12\text{ kg}^{-1}$ ,<sup>7</sup> and  $\$12\text{--}16\text{ kg}^{-1}$ ,<sup>8,9</sup> among others. The cost of green H<sub>2</sub> produced depends on several factors such as module and tracker cost, electrolyser stack cost, balance of system (BOS) and balance of plant (BOP) cost, operation and maintenance (O & M) cost and system efficiency.<sup>7,10,11</sup> Out of all these factors the system efficiency or in other words the solar to hydrogen (STH) efficiency directly influences all the other factors and can lead to significant reduction in size of PV and electrolyser plants.<sup>10</sup> Silicon PV cells are close to reaching their theoretical efficiencies of  $\sim 30\%$  which means that there is not much scope of increasing the STH efficiency with silicon PV.<sup>12</sup> Unlike silicon PV, concentrator photovoltaic cells (CPV) based on III-V group elements have already reached a much higher efficiency of  $\sim 47\%$  (4J cell)<sup>13</sup> and theoretically can reach over 80% efficiency.<sup>14-16</sup> At a modular level, 43.4%<sup>16</sup> and 43%<sup>17</sup> efficient CPV modules have been demonstrated with a projected modular efficiency of 47% by 2035.<sup>16-18</sup> Moreover they can operate at high light concentrations ( $>1000$  suns) largely compensating for the higher manufacturing cost.<sup>16</sup>

The high efficiency of CPV cells has encouraged researchers to explore CPV-electrolysis (CPV-E) setups in recent years. For instance, Chang and co-workers reported a STH efficiency of  $\sim 20.6\%$  using a single junction GaAs PV cell coupled to a proton-exchange-membrane (PEM) electrolyser using a DC-DC convertor.<sup>19</sup> Nakamura and co-workers reported a STH efficiency of 24.4% using a CPV-E system, without the use of power

Hydrogen Platform, SABIC-CRD, King Abdullah University of Science and Technology (KAUST), Thuwal 23955, Saudi Arabia. E-mail: [mohd.khan1@ucalgary.ca](mailto:mohd.khan1@ucalgary.ca); [IdrissH@SABIC.com](mailto:IdrissH@SABIC.com)

† Electronic supplementary information (ESI) available. See DOI: [10.1039/d0se01761b](https://doi.org/10.1039/d0se01761b)



electronics.<sup>20</sup> The power matching was done by optimizing the ratio of the number of electrolysers to CPV cells. The highest STH efficiency ( $\sim 31\%$ ) was reported on a laboratory scale through direct coupling of two PEM electrolysers with one CPV cell, operating at 42 suns.<sup>21</sup> All these previous reports coupled CPV cells with PEM electrolysers which are expensive with high stack and BOP costs.<sup>11,22</sup> Moreover, there are no reports on techno-economic analysis (TEA) of CPV-E systems, to investigate the effect of using high efficiency CPV cells on the cost of  $\text{H}_2$  produced, which was the primary motivation to move away from silicon solar cells.

In this work, we give experimental evidence of the potential of CPV cells for achieving high STH efficiency and subsequently analyse the effect of efficiency and economy of scale on  $\text{H}_2$  cost.

(1) Specifically, we used triple junction (3J) InGaP/InGaAs/Ge CPV cells connected to alkaline electrolysers. With appropriate power matching, and without a DC-DC converter, it was possible to achieve a STH efficiency of 28% under 41 suns, which is the highest efficiency reported to date for PV cells coupled with alkaline electrolysers.

(2) Using this as a base case, we carried out a TEA analysis of cost of  $\text{H}_2$  produced assuming a commercial CPV farm (module efficiency  $\sim 41\%$ ) coupled with an alkaline electrolyser plant (electrolyser efficiency  $\sim 70\%$ ), thus operating at 28% plant or STH efficiency. The levelized cost of  $\text{H}_2$  under these base case conditions was  $\sim 5.9 \text{ \$ kg}^{-1}$  and expected to go down to  $5.6 \text{ \$ kg}^{-1}$ , at a STH efficiency of 31.5%. In comparison, the cost of hydrogen when using silicon PV modules (module efficiency  $\sim 17.5\%$ ) was calculated to be  $\sim 4.9 \text{ \$ kg}^{-1}$ .

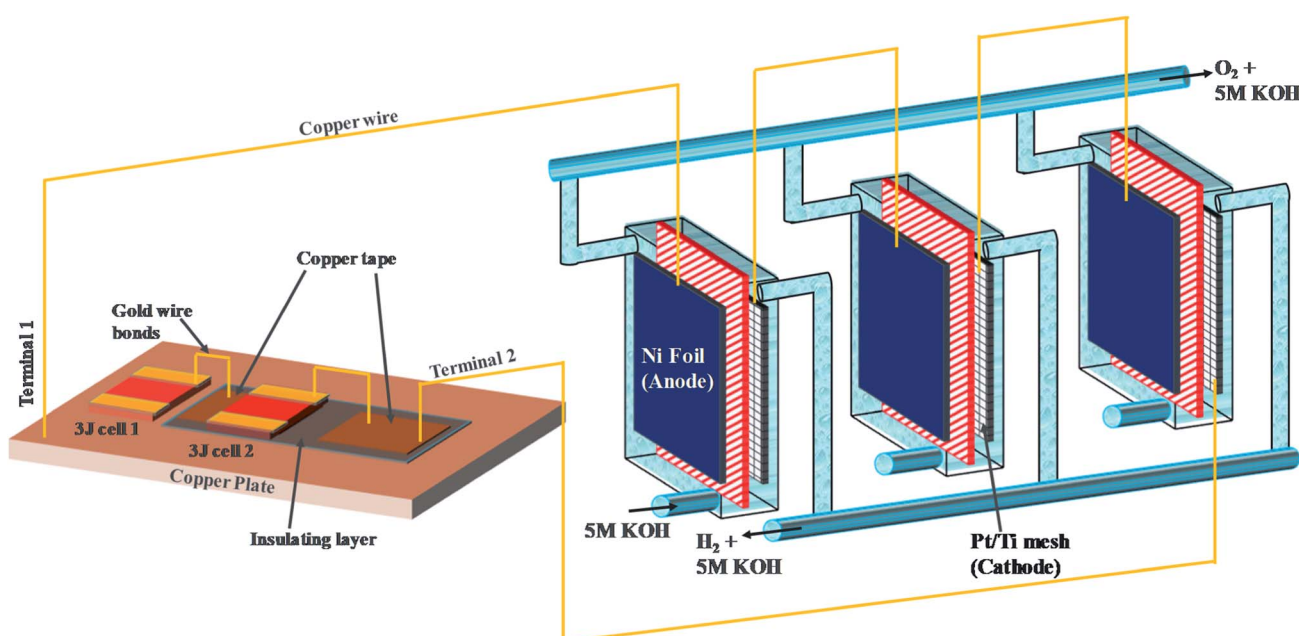
(3) We have also projected the cost of CPV modules, trackers and associated  $\text{H}_2$  as a function of cumulative installed capacity. At a learning rate of 18%, the cost of  $\text{H}_2$  from CPV-E setups could go down to  $2.65 \text{ \$ kg}^{-1}$  if the cumulative installed capacity exceeds  $>100 \text{ GW}$  in a range like silicon PV cells.

We hope that the experimental results obtained (STH efficiency = 28%), stable performance, followed by TEA, will encourage researchers, governments, and companies to explore CPV-E setups for large-scale green  $\text{H}_2$  production.

## 2. Methodology

### a. PV-E setup

The PV-E experimental setup was designed as shown in Scheme 1. Alkaline electrolysers were fabricated using poly(methyl methacrylate) (PMMA) sheets, ideal for use under alkaline conditions. An alkaline anion exchange membrane (Sustainion® 37-50) with area  $\sim 12.25 \text{ cm}^2$  was used for ion transfer and gas separation. Nickel foil (Alfa Aesar, 99.5% purity, 0.25 mm thick) was used as the anode. A platinum film (Kurt J. Lesker, 99.99% pure target, 10 nm thick) was sputtered onto both sides of a porous titanium mesh used as the cathode. The geometric area of the anode and cathode was the same as that of the anion exchange membrane. Triple junction (3J) GaInP/GaInAs/Ge CPV cells ( $3.0 \times 3.0 \text{ mm}^2$ ) from Azure Space (type 3C44C) were used as the photoabsorbers. The first CPV cell was mounted onto an air-cooled copper plate using silver paste (High Purity Silver paint, SPI-Paint, 43% Ag solid, bulk resistivity  $3 \times 10^{-7} \Omega \text{ m}$ ) due to its high thermal and electrical



**Scheme 1** The PV-electrolysis setup consists of two-3J CPV cells (each is composed of GaInP/GaInAs/Ge CPV cells ( $3.0 \times 3.0 \text{ mm}^2$ )) connected in series to three alkaline electrolysers, also connected in series. Each alkaline electrolyzer is composed of ca. 10 nm Pt particles deposited on both sides of a Ti mesh (Pt/Ti mesh) as the cathode and a  $\text{Ni(OH}_2\text{)}/\text{Ni}$  as the anode. The electrolyte (5 M KOH solution) is recirculated. Terminal 1: back side of the cells (+), and terminal 2: front side of the cell (-). Light at 41-sun concentration illuminated the cells, without the use of Fresnel lenses.



conductivity. The silver paste was dried in an oven at 70 °C for 2 hours. To make a series connection, the second CPV cell was insulated from the copper plate using a polyimide tape. The electrical connections as shown in the schematic were realised using ball wire bonding with 25 µm gold wire (HB16, TPT Wire Bonder GmbH & Co). The two CPV cells are coupled with three alkaline electrolyzers connected in series using copper wires. The electrolyte (5 M KOH) flow was split between the three electrolyzers and H<sub>2</sub>/O<sub>2</sub> gases were collected and measured volumetrically (their purity was independently confirmed with gas chromatography (GC) as a routine check).

### b. Techno-economic analysis

To estimate the return on capital investment for the development of a CPV-E facility, a discounted cash flow spreadsheet was developed to calculate the capital expenditure (CAPEX), annual operating expenditure (OPEX) and revenue over the project lifetime (see ESI† tables). It was assumed that land acquisition, CAPEX allocation and construction of the plant were completed in the first three years, with plant operation beginning in the fourth year. A nominal interest rate (NIR) of 12% was used in the study, while the working capital was assumed to be 15% of the capital investment. A plant lifetime of 20 years was taken based on the typical lifetime of PV cells while the cost of storage and transportation of hydrogen was not considered in this study.<sup>7,23</sup> The analysis was designed for a plant based in the city of Tabuk in Saudi Arabia, operating for 9.1 hours per day without grid support and for a production capacity of 50 ton H<sub>2</sub> per day at a pressure of 20 bars. The region of Tabuk was chosen for its high daily average sunshine (9.1 hours),<sup>24</sup> a low population density (6 km<sup>-2</sup>), and high direct normal irradiance (DNI) of ~7.37 kW h m<sup>-2</sup>.<sup>25</sup> The electricity price needed to run pumps, power electronics and other utilities was taken at 0.05 \$ kW<sup>-1</sup> h<sup>-1</sup> (unless otherwise stated). The process contingency in this analysis uses 20% of direct costs due to the greater uncertainties in the system configuration.<sup>26</sup> The indicated process

and economic assumptions are summarized in Table 1 (more details are given in the ESI† tables). The capital and utility costs of compressors and pumps were modelled using Aspen Plus. The leveled cost of hydrogen (LCOH) also known as the minimum selling price (MSP) was calculated by adjusting its value such that the net present value (NPV) of the capital and operating expenses and product revenue are summed to zero (eqn (1)–(3)).

$$\text{Operating cost present value} = \sum_{i=1}^n \frac{\text{Operating cost}_i}{(1+r)^i} \quad (1)$$

Product revenue present value

$$= \sum_{i=1}^n \frac{\text{Product revenue}_i(\text{LCOH})}{(1+r)^i} \quad (2)$$

$$\text{NPV} = 0 = \text{product revenue PV} - (\text{operating cost PV} + \text{capital expenses}) \quad (3)$$

*i*: number of years, *r*: required return or discount rate, and *n*: 20 years.

## 3. Results and discussion

### a. Experimental results

Fig. 1(a) shows the current–voltage (*I*–*V*) characteristics of the InGaP/InGaAs/Ge 3J CPV cell (3 × 3 mm<sup>2</sup>) from Azur Space under one and multiple suns up to 41-sun illumination. The cell was mounted onto an air-cooled copper plate, maintaining the temperature at ~25 °C. An Asahi Spectra 320 W solar simulator (350–1800 nm) was used as the light source and the irradiation was adjusted by the distance to the device and the power of the solar simulator. The one sun light flux was verified using a pre-calibrated monocrystalline silicon reference cell (Newport, 91150-KG5). Following a standard method for characterizing CPV cells, we used the ratio of the short circuit currents to confirm that the cell was illuminated with 41 suns. Under 41 suns (obtained directly from solar simulation without the use of external light concentrators such as Fresnel lenses), the short circuit current and open-circuit voltage (*V*<sub>oc</sub>) were 56.50 mA and 2.93 V, respectively. At the maximum power point (MPP), the voltage (*V*<sub>MPP</sub>) and current (*I*<sub>MPP</sub>) were 2.70 V and 55.62 mA, respectively. The calculated fill factor (FF) and solar-to-electricity or PV cell efficiency was 0.90 and 40.7% under these operating conditions. More information on the Azur space cells is given in Fig. S1 and S2 of the ESI.† We have opted not to use Fresnel lenses in this work to minimize losses, and therefore the highest possible sun concentration obtained directly from the solar simulator was 41 suns. To increase the sun light flux the use of Fresnel lenses is needed and with them associated losses which depend very much on their materials nature (quality) and configuration.<sup>27</sup> We have previously observed that the use of Fresnel lenses as light concentrators led to additional optical losses up to 30%<sup>5</sup> without optimization, although further improvement was made possible, dropping the loss to *ca.* 15%.<sup>4</sup>

Table 1 Process and economic parameters used for PV-E plants

Location	Tabuk, KSA
<b>Process parameters</b>	
Total production (ton per day)	50
Sunshine hours (hours per day) <sup>24</sup>	9.1
H <sub>2</sub> production rate (ton per h)	5.49
Annual working days (days per year)	333
H <sub>2</sub> production rate (ton per year)	16 650
Solar irradiation (kW h m <sup>-2</sup> ) <sup>25</sup>	7.37
Energy per kg of H <sub>2</sub> (kW h kg(H <sub>2</sub> ) <sup>-1</sup> ) – LHV	32.66
Required electricity for utilities (kW h per ton H <sub>2</sub> )	161
<b>Economic parameters</b>	
Plant lifetime (years) <sup>7,23</sup>	20
Discount rate ( <i>r</i> ) (%)	12
Land cost (\$ km <sup>-2</sup> ) <sup>26</sup>	\$123 497.00
CO <sub>2</sub> credit (\$ per ton CO <sub>2</sub> ) <sup>11,28,29</sup>	50
O <sub>2</sub> credit (\$ per ton O <sub>2</sub> ) <sup>30</sup>	40
Electricity price (\$ kW <sup>-1</sup> h <sup>-1</sup> )	0.05
Contingency	20%



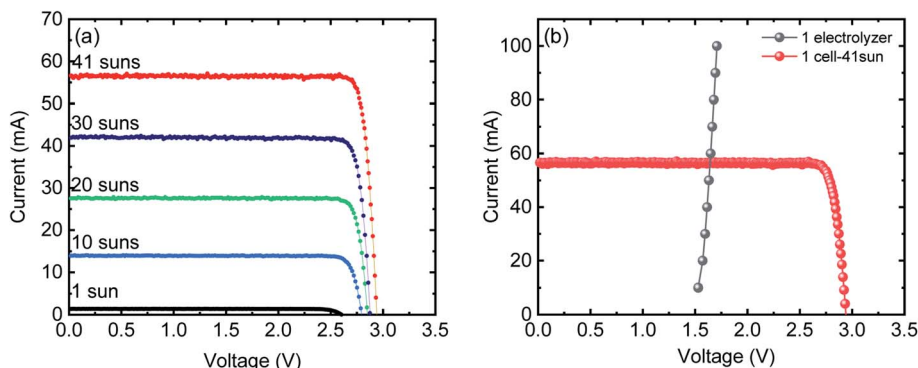


Fig. 1 (a)  $I$ – $V$  characteristics of the InGaP/InGaAs/Ge 3J CPV cell ( $3 \times 3 \text{ mm}^2$ ) from Azur Space under one sun to 41-sun illumination (note the linearity of the current as a function of light concentration). (b)  $I$ – $V$  curve of single alkaline electrolyser (grey) generated using CP measurements overlapped with the  $I$ – $V$  curve of the 3J CPV cell (red) under 41 suns (without the use of Fresnel lenses).

Fig. 1(b) overlaps the  $I$ – $V$  characteristics of a single alkaline electrolyser and the CPV cell. The  $I$ – $V$  curve of the electrolyser was generated using chrono-potentiometry (CP) measurements performed at different current densities. The cross-point of the electrolyser  $I$ – $V$  curve and the solar cell  $I$ – $V$  curve is the system coupling point and specifies the operating voltage ( $V_{OP}$ ) and current ( $I_{OP}$ ) of the system, which was  $\sim 1.66 \text{ V}$  and  $56.3 \text{ mA}$  respectively. Since the  $V_{MP}$  of the CPV cell under 41 suns is  $\sim 2.70 \text{ V}$ , there is an additional  $1.04 \text{ V}$  that results in energy wasted as heat rather than stored in  $\text{H}_2$  chemical bonds. Based on the operating current ( $I_{OP}$ ), the maximum STH efficiency of the system calculated using eqn (4) was found to be  $\sim 18.7\%$  based on 100% faradaic efficiency ( $\eta_F$ ).

$$\text{STH} = \frac{(J_{sc}(\text{mA cm}^{-2})) \times (1.23 \text{ V}) \times (\eta_F)}{P(\text{mW cm}^{-2})} \quad (4)$$

While the additional  $1.04 \text{ V}$  is not enough to run another electrolyser, the limitation can be overcome by coupling multiple PV and/or electrolyser units connected in series, to match the voltage characteristics of the components.<sup>20</sup>

Fig. 2(a) shows the  $I$ – $V$  characteristics of two InGaP/InGaAs/Ge 3J CPV cells ( $3 \times 3 \text{ mm}^2$ ) connected in series, under 41-sun

illumination. As expected upon using two cells in series, the current remained unchanged, but the total voltage increased. At the MPP, the  $V_{MP}$  and  $I_{MP}$  were  $5.29 \text{ V}$  and  $55.18 \text{ mA}$ , respectively. The configuration of the three electrolyzers in terms of electro-catalysts, membranes and electrolyte conductivity was designed to match the characteristics of the two cells. Overlapping with the  $I$ – $V$  curves of the three alkaline electrolyzers connected in series resulted in a  $V_{OP}$  and  $I_{OP}$  of  $5.02 \text{ V}$  and  $56.21 \text{ mA}$ , respectively. Thus, it is possible to utilize the extra voltage from the two cells and run a third electrolyser. Fig. 2(b) shows the  $\text{H}_2$  and  $\text{O}_2$  production rates from the system, presented in Scheme 1, under 41 sun-illumination. There was stoichiometric production of  $\text{H}_2$  and  $\text{O}_2$  in  $2 : 1$  ratio at a STH efficiency of  $\sim 28\%$ , which was calculated using eqn (5):

$$\text{STH} = \frac{\text{Power from hydrogen produced}}{\text{Power of light incident onto the CPV cells}} \quad (5)$$

## b. TEA results for the base case

A STH efficiency of 28% is the highest reported for PV cells coupled to alkaline electrolyzers. As mentioned earlier, the STH efficiency is an important driver for researchers and directly

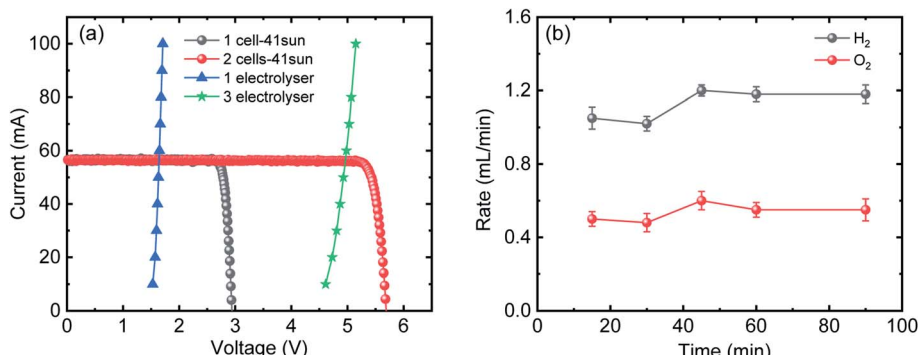


Fig. 2 (a)  $I$ – $V$  curves of one (grey) and two 3J CPV cells (red) connected in series under 41-sun illumination overlapped with  $I$ – $V$  curves of single (blue) and three (green) alkaline electrolyzers connected in series. (b)  $\text{H}_2$  and  $\text{O}_2$  production rates from three alkaline electrolyzers connected in series. Power is supplied from two CPV 3J cells connected in series under 41-sun illumination (without the use of Fresnel lenses to minimize further losses) as shown in Scheme 1.



Table 2 CPV, c-Si PV and electrolyser parameters used for the base case study

PV parameters	CPV	Silicon
Power needed for solar farm (kW)	256 357.92	256 357.92
Module efficiency (%)	41	12% ( $17.5 \times 0.685$ )
Sunlight concentration	820	1
Tracker	Dual axis	Single axis
Land or PV packing factor <sup>31</sup>	4	3
Module and tracker cost (\$ W <sup>-1</sup> )	0.72 (ref. 32)	0.50 (ref. 33 and 34)
Design, labour, permitting and installation (\$ W <sup>-1</sup> )	0.43	0.30
PV inverter cost (\$ W <sup>-1</sup> ) <sup>34</sup>	0.08	0.07
PV O & M cost (USD per kW h) <sup>34</sup>	0.008	0.008
<b>Electrolyser plant parameters</b>		
Electrolyser plant size (kW)	256 357.92	
Electrolyser efficiency (%) <sup>9,11</sup>	70%	
Electrolyser O & M (% of total uninstalled CAPEX) <sup>7,23</sup>	3%	
Stack cost (\$ kW <sup>-1</sup> ) <sup>22</sup>	272	
Balance of plant (BOP) capital cost (\$ kW <sup>-1</sup> ) <sup>11,22</sup>	272	
H <sub>2</sub> loss due to separation	3.0%	
Electrolyser installation factor <sup>35</sup>	12.0%	
Electrolyte needed (ton per ton H <sub>2</sub> )	10	
Electrolyser replacement factor <sup>7,35</sup>	1.5%	

affects H<sub>2</sub> cost. Using this as a base case, we have conducted TEA for green hydrogen production using a CPV-E system working at an STH efficiency of 28.7%. As a reference, the same analysis was done for H<sub>2</sub> produced using conventional c-Si PV technology. The process and economic parameters were identical in both cases; these are summarized in Table 1.

Table 2 shows the CPV farm and electrolyser plant parameters used for the base case study. Based on a H<sub>2</sub> production capacity of 50 ton per day, the PV farm and electrolyser plant were sized at ~256.3 MW based on an electrolysis efficiency of 70%, and 9.1 hours daily operation, using eqn (6).

modules are known to maintain >90% of their efficiency throughout the day while c-Si modules with single axis tracking only maintain their efficiency of ~60–70% of the day.<sup>38,39</sup> Moreover, silicon PV cells are temperature-sensitive with a temperature coefficient of about  $-0.5\%$  per  $^{\circ}\text{C}$ , which means that for every degree above 25° it loses 0.5% of performance.<sup>40,41</sup> Thus, for accuracy, the average module efficiency of c-Si was taken as 12% ( $17.5 \times 0.685$ ). The average packing factor or land factor was taken as 4, which is the standard for CPV farms with dual axis trackers and 3 for c-Si farms with single axis tracking.<sup>31</sup> This land factor is the ratio of actual land area to PV array area

$$\text{Power required (kW)} = \frac{\text{H}_2 \text{ production rate (kg per day)} \times \text{energy per kg of H}_2 \text{ (kW h per kg(H}_2\text{))}}{\text{Electrolysis efficiency} \times \text{sunshine hours(h per day)}} \quad (6)$$

The CPV module cost as a function of efficiency was taken from an analysis performed by the National Renewable Energy Laboratory (NREL) in 2015,<sup>32</sup> operating at high concentrations of  $\sim 830\times$  and was further verified with industrial input/private communication from CPV module manufacturers (BSQ, Spain).<sup>32,36</sup> The cost of the dual axis tracker needed for CPV modules was taken at  $\sim 50\%$  of the module cost, based on industrial input/private communication (BSQ, Spain).<sup>36</sup> The cost of labour, design, permitting and interconnection of the PV solar farm was taken as an average from various reported installed projects.<sup>37</sup> At a module efficiency of 41%, the CPV module cost would be  $\sim 0.48 \text{ } \$ \text{ W}^{-1}$  with a dual axis tracker cost of  $0.24 \text{ } \$ \text{ W}^{-1}$ .<sup>32</sup> In contrast highly efficient (17.5%) c-Si modules are much cheaper with module costs at  $0.3 \text{ } \$ \text{ W}^{-1}$ <sup>33</sup> and tracker costs of  $0.2 \text{ } \$ \text{ W}^{-1}$ .<sup>33,34</sup> It is important to note here that CPV

and encompasses space requirements for pumps, compressors, heat exchangers, a control room, and access roads.

The total CAPEX of alkaline electrolyzers was taken at  $\sim 544 \text{ } \$ \text{ kW}^{-1}$ , considering multi stack systems operating at full load hours.<sup>22</sup> The stack cost contributes  $\sim 50\%$  to the electrolyser CAPEX, while 50% is for BOP which consists of a gas management system, electrolyte delivery system, thermal management and power electronics.<sup>11</sup> For the base case scenario, the electrolyser replacement factor was calculated assuming a change of the electrolyser stack every 7 years, which means two changes throughout a plant lifetime of 20 years.<sup>7,35</sup> The stack replacement cost is taken as 15% of the total electrolyser CAPEX; an annual electrolyser replacement factor of  $\sim 1.5\%$ .<sup>7</sup>

Table 3 and Fig. 3 present the base case results of the TEA analysis following the assumptions listed in Table 2. The total



Table 3 Base case results for the studied systems

CAPEX	CPV	Silicon PV
Total PV cost (\$)	\$315 832 967.03	\$225 594 976.45
Total electrolyser capital (\$)	\$156 193 758.24	\$156 193 758.24
Gas processing (\$)	\$4 143 572.97	\$4 143 572.97
Electrolyte processing (\$)	\$29 306.58	\$29 306.58
Land cost (\$)	\$381 375.86	\$977 275.64
Contingency (%)	\$94 858 545.11	\$77 387 777.97
Total CAPEX (\$)	\$571 439 525.79	\$464 326 667.85
<b>OPEX</b>		
Annual PV maintenance (\$ per year)	\$18 662.86	
Compressor (\$ per year)	\$393 477.73	
Water pump (\$ per year)	\$20 755.22	
Annual water cost (\$ per year)	\$216 450.00	
O & M of electrolyser (\$ per year)	\$4 183 761.38	
Annual electrolyser replacement (\$ per year)	\$2 342 906.37	
Annual electricity cost for utilities (\$ per year)	\$134 032.50	
Annual staff cost (\$ per year)	\$1 598 400.00	
Total OPEX (\$ per year)	\$8 908 446.06	
LCOH (\$ per kg)	\$5.9	\$4.9

CAPEX of the CPV and electrolyser plants was \$571 439 525.79, with the CPV solar farm cost being the dominant factor (55.27%) due to the current high costs of CPV modules. The CAPEX costs for the c-Si solar farm were less at \$464 326 667.85 primarily due to cheaper modules. The module cost is determined by several factors out of which the dominant ones are the module efficiency, cell costs ( $\$/m^2$ ), manufacturing yield, assembly costs and scale of manufacturing.<sup>32</sup> While CPV cells are twice efficient compared to silicon cells, they are more expensive ( $\sim 12\ 000\ \$/m^2$  versus  $\sim 70\text{--}80\ \$/m^2$ ).<sup>32,42</sup> In recent years with the commercialization of high concentration technology (>800 suns), the effect of CPV cell cost has diminished. Currently the biggest hurdle for CPV modules is the scale of manufacturing which will also reduce assembly costs. The role of economy of scale will be discussed in Fig. 4. Another major difference in CAPEX costs is the land costs of  $\sim \$381,375.86$  for a CPV farm versus  $\$977 275.64$  for a c-Si farm, arising due to the lower efficiency c-Si modules. Since the land is very cheap, because of the location (Table 1), the total land cost is a very small fraction (<1%) of the total CAPEX for both technologies and does not affect the final cost of  $H_2$  a great deal. However, the availability of land and its cost in other locations might be a critical factor, in densely populated areas, with the c-Si solar

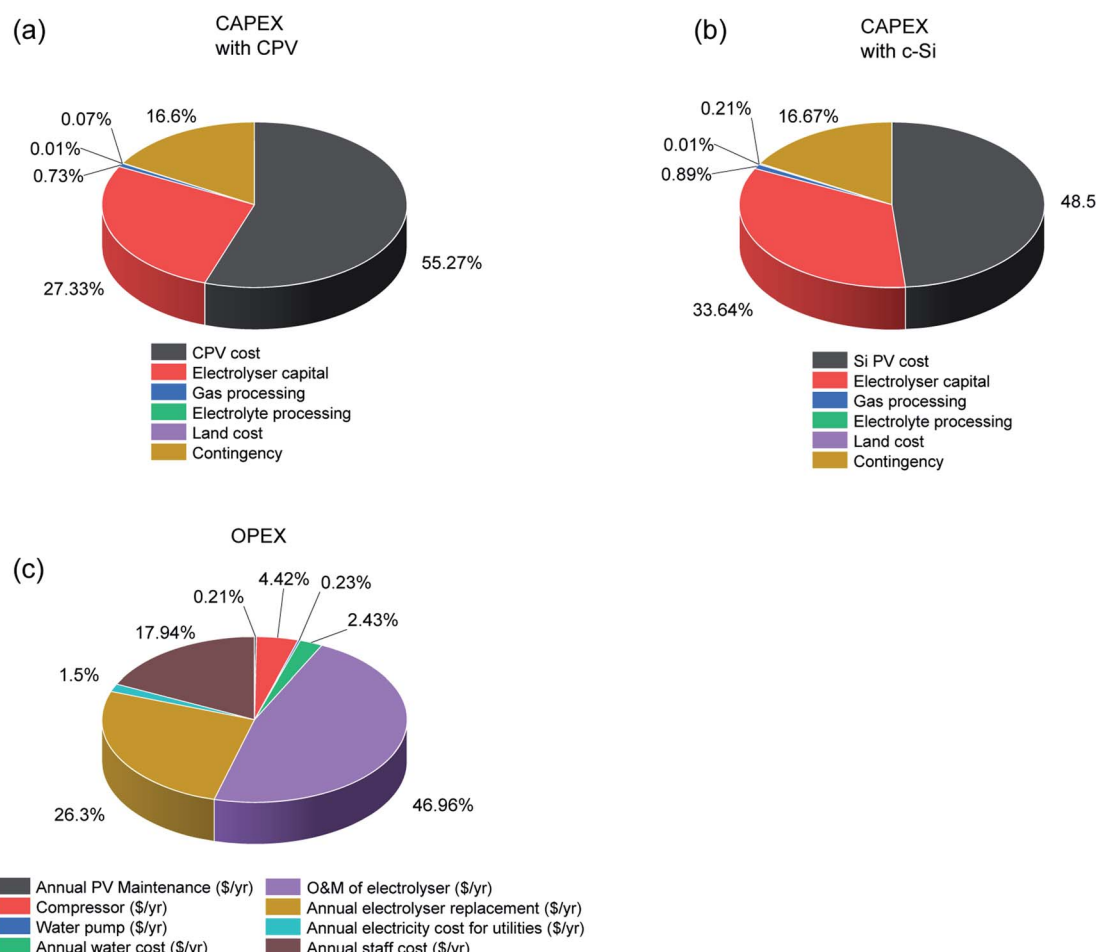


Fig. 3 Breakdown of total capex for a CPV (a) and c-Si PV (b) powered electrolysis process to produce 50 tons  $H_2$  per day using the assumptions listed in Tables 1 and 2. (c) Annual OPEX for both technologies i.e. CPV-E and c-Si PV-E.



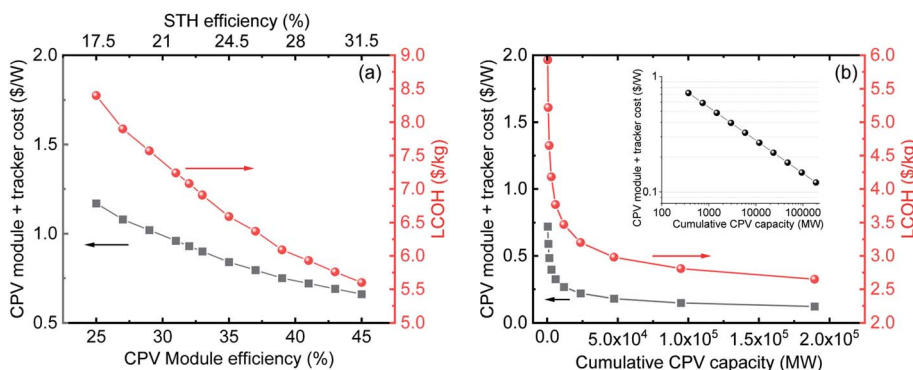


Fig. 4 (a) Module + tracker costs (left) and cost of  $\text{H}_2$  (right) as a function of CPV module efficiency (bottom) and STH efficiency (top). (b) Module + tracker costs (left) and cost of  $\text{H}_2$  (right) as a function of projected cumulative CPV capacity (bottom). For both projections, the electrolyser efficiency, CAPEX and OPEX were kept constant as mentioned in Tables 2 and 3.

farm needing about 2.5 times more land area than the CPV farm.

The annual OPEX of \$8 908 446 is identical for both systems; with electrolyser O & M and electrode replacement cost the dominant factors at 46.96% and 26.3%, respectively. Currently, the electrolyser market is also relatively small with total worldwide installed capacity in the MW scale.<sup>11</sup> With increase in production and global cumulative installations, the electrolyser O & M costs are expected to drop.<sup>11</sup> The electrode replacement costs will come down with development of catalysts with improved stability and efficiency. The effect of catalyst lifetime on the  $\text{H}_2$  price is discussed in Fig. 5. The revenue stream mainly consists of income from  $\text{H}_2$  (~91%) with a small fraction from  $\text{O}_2$  and  $\text{CO}_2$  credit (~9%) (the  $\text{CO}_2$  credit is based on the  $\text{CO}_2$  released while making hydrogen from methane (5.5 times the amount of hydrogen per weight) without considering process energy consumption as per the equation:  $\text{CH}_4 + 2\text{H}_2\text{O} \rightarrow 4\text{H}_2 + \text{CO}_2$ ). After calculating the CAPEX, OPEX and revenue, we determined the LCOH using a discounted cash flow method and the economic assumptions and parameters listed in Table 1. The LCOH at which the NPV is zero was ~5.9 \$  $\text{kg}^{-1}$  for the CPV-E process and ~4.9 \$  $\text{kg}^{-1}$  for the c-Si PV-E setup (Table 3).

### c. Sensitivity analysis

To understand the effect of various parameters on the LCOH, a sensitivity analysis was performed. We first analysed the effect of two factors critical for CPV technology. These are (i) CPV module efficiency and (ii) economy of scale or cumulative installed capacity. As mentioned earlier, CPV cells have the potential to reach a theoretical efficiency of over 80%; and 60% cell efficiency is a real possibility in the next few years. The analysis is for CPV module efficiencies ranging from 25 to 45% as 43.4%<sup>16</sup> and 43%<sup>17</sup> efficient modules have already been demonstrated on a laboratory scale with projections of a 47% efficient module commercially available by 2035.<sup>16-18</sup> A higher efficiency means higher output power per unit area which directly translates into lower cost (\$  $\text{W}^{-1}$ ) or in other words, a smaller cell area is needed to reach the same output power. Therefore, it is important to analyse the effect of increase in CPV

module efficiency on the leveledized cost of  $\text{H}_2$ . Using an analysis by NREL on the effect of efficiency on CPV module costs, we calculated the cost of  $\text{H}_2$  at different module efficiencies or STH efficiencies.<sup>28</sup> For these calculations, we have assumed a fixed electrolyser efficiency of 70% and costs, as listed in Table 2. Fig. 4(a) shows the dependence of the “CPV module plus tracker cost” as well as the “LCOH” (y-axes) on the “CPV module efficiency” and “STH efficiency” (x-axes). We notice that the efficiency of the system reduces the total CAPEX in different ways. In addition to the expected reduction in modular costs a noticeable reduction in trackers cost, labour, installation, maintenance and of the land costs occurs. This results in reduction in the cost of  $\text{H}_2$  from ~8.4 \$  $\text{kg}^{-1}$  at a STH efficiency of 17.5% to ~5.6 \$  $\text{kg}^{-1}$  at 31.5% STH efficiency as seen in Fig. 4(a).

The analysis in Fig. 4(a) is based on the effect of increasing efficiency on lowering module cost and LCOH. The decrease of the CPV module + tracker cost with increasing the CPV module efficiency is primarily due to the use of fewer materials, as indicated above. With further momentum on the use of CPV technology, significant cost reductions can be expected due to the economy of scale. As an example, in the last 40 years c-Si technology has seen prices going down from ~80 \$  $\text{W}^{-1}$  to ~0.3 \$  $\text{W}^{-1}$  as cumulative capacity increased from ~5 MW to

Table 4 Projected CPV module plus tracker costs based on cumulative capacity and a LR of 18%

Projected CPV cumulative capacity (MW)	Projected CPV module + tracker cost (\$ $\text{W}^{-1}$ )
370 (current - 2020)	0.72
740	0.59
1480	0.48
2960	0.40
5920	0.32
11 840	0.27
23 680	0.22
47 360	0.18
94 720	0.15
189 440	0.12



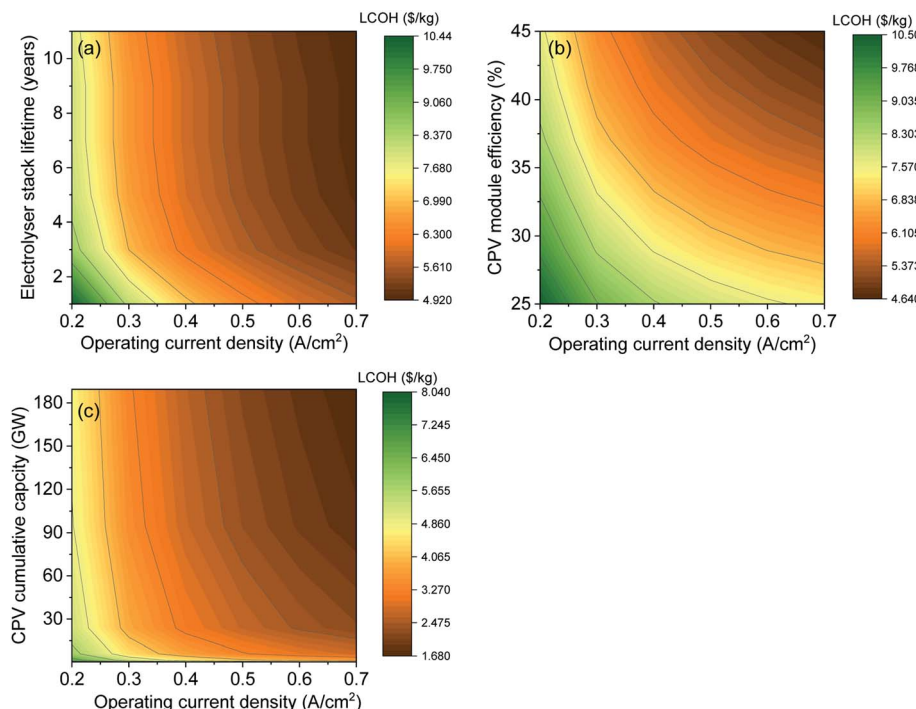


Fig. 5 Contour plots showing the sensitivity of  $\text{H}_2$  cost to: (a) electrolyser stack lifetime, (b) CPV module efficiency and (c) CPV cumulative installed capacity *versus* operating current density of the electrolyser.

500 GW, leading to a learning rate (LR) of  $\sim 28\%$ .<sup>33</sup> In the last year, Si-PV module prices have reached a plateau while CPV has still a very large price drop potential. CPV systems have seen a LR of  $\sim 18\%$  which can be used to project module costs as cumulative capacity increases.<sup>43</sup> Currently, the cumulative capacity of CPV farms is only around 370 MW,<sup>16</sup> with module and tracker costs of  $\sim 0.72 \text{ \$ W}^{-1}$ . Using this as a starting point and LR of 18% we have projected prices to go down to  $\sim 0.12 \text{ \$ W}^{-1}$  if the cumulative capacity increases up to  $\sim 189 \text{ GW}$  (see Table 4 and inset of Fig. 4(b)). The CPV modules were kept constant for these projections. Based on these projected costs, we have also calculated the LCOH as shown in Fig. 4(b). We observe a significant reduction in LCOH from  $5.9 \text{ \$ kg}^{-1}$  currently to  $\sim 2.6 \text{ \$ kg}^{-1}$  when module prices go down to  $\sim 0.12 \text{ \$ W}^{-1}$ . It is important to note that the projections presented in Fig. 4 are based solely on reduction in CPV module prices without considering the foreseen drop in electrolyser costs. The combined effect of improvement in CPV and electrolyser performance on LCOH is analysed in the next section.

To analyse the sensitivity to electrolyser CAPEX cost, we have changed the model to be sensitive to operating current density by determining the electrolyser stack cost per unit area. This is calculated using a reference stack cost of  $272 \text{ \$ kW}^{-1}$ , operating conditions at  $0.4 \text{ A cm}^{-2}$  and  $1.7 \text{ V}$  (the base case) corresponding to an installed cost of  $\$1850 \text{ m}^{-2}$ .<sup>44</sup> Depending on the operating current density and the electrolyser area, the capital cost of the electrolyser changes. Fig. 5(a) shows the effect of LCOH as a function of electrolyser stack lifetime and electrolyser operating current density at 41% CPV module efficiency. The stack lifetime affects the electrolyser OPEX while the

operating current density affects the electrolyser CAPEX. The results show that LCOH is sensitive to both operating current density and stack lifetime when the lifetime is below 3 years. The impact of stack lifetime on the LCOH is less pronounced after 4 years, where it is more affected by the change in current density or in other words the size of the electrolyser. Moreover, the effect of changing the performance of both the CPV solar farm and the electrolyser on the LCOH is given in Fig. 5(b). Both parameters have almost an equal impact on the LCOH, where the cost drops to  $4.64 \text{ \$ kg}^{-1}$  when the CPV module efficiency and the operating current density are at 45% and  $0.7 \text{ A cm}^{-2}$ , respectively. Finally, the effect of CPV installed cumulative capacity and stack current density on the LCOH is shown in Fig. 5(c). The graph summarizes the importance of both CPV and electrolyser CAPEX on  $\text{H}_2$  cost. When the cost of CPV modules keeps decreasing at a LR of  $\sim 18\%$ , LCOH can be  $< 2 \text{ \$ kg}^{-1}$  at an installed CPV cumulative capacity of  $> 180 \text{ GW}$  and an operating current density of  $0.7 \text{ A cm}^{-2}$ . The effect of grid electricity cost for 24 hours operation on the LCOH is given in the ESI.<sup>†</sup>

## 4. Conclusions and outlook

The present experimental work shows that a stable system with a STH efficiency of 28% can be obtained upon optimising the configuration of CPV cells (40.7% efficient) and available alkaline electrolyzers (70% efficient). Detailed TEA analysis showed that despite the high cost of these CPV cells, the LCOH with CPV solar farms, today, can approach that obtained using c-Si solar farms. Because commercial c-Si solar cells have neared



saturation, we have carried out a sensitivity analysis of several factors affecting both CPV and alkaline electrolyser systems. These included the CPV module efficiency, installed capacity, electrolyser stack lifetime and operating current density. Results indicate that when the installed capacity of CPV technology matches that of silicon and when electrolyser's operating current density reaches  $\sim 0.7 \text{ A cm}^{-2}$ , the levelized cost of  $\text{H}_2$  from CPV-electrolysis systems can drop below  $\$2 \text{ kg}^{-1}$ . The present cost of hydrogen from steam methane reformers with  $\text{CO}_2$  sequestration is between  $\$1.2$  and  $\$2.8 \text{ kg}^{-1}$ .<sup>6</sup>

Hydrogen can be produced from water with high efficiency and production rates. The considerable increase in efficiency as seen in this work puts STH efficiency at par with other practical engines. Like any technology, the one presented here will see its cost dropping down with time once in use and like any breakthrough technology; it can only be brought to life with strong incentives. In recent years, the silicon PV industry experienced a large price drop of more than 80% mostly from subsidized industries that could sell products with little to no profit. On the other hand, CPV has suffered from a lack of a dedicated supply chain, which has forced many companies to develop and produce most of the components (trackers, modules, *etc.*) themselves. We hope that these results and cost analysis will encourage researchers, governments, and companies to explore CPV-electrolysis for commercial  $\text{H}_2$  production. The main incentive, in the short term, may not be wealth but the environment; and this would bring with time the needed ingredients for progress and prosperity.

## List of abbreviations

IRR	Internal rate of return
OPEX	Operating expenditure
CAPEX	Capital expenditure
PV	Photovoltaic
CPV	Concentrated photovoltaic
LCOH	Levelized cost of hydrogen
BOS	Balance of system
BOP	Balance of plant
DI	De-ionized water
O & M	Operation and maintenance
PEM	Polymer electrolyte membrane
STH	Solar to hydrogen efficiency
NPV	Net present value
MSP	Minimum selling price
FF	Fill factor
PMMA	Poly(methyl methacrylate)
GC	Gas chromatography
DNI	Direct normal irradiance
$\eta_F$	Faradaic efficiency
$V_{OP}$	Operating voltage
$I_{OP}$	Operating current
$V_{MMP}$	Voltage at maximum power point
$I_{MMP}$	Current at maximum power point
3J	Triple junction
NREL	National renewable energy laboratory

## Conflicts of interest

There are no conflicts to declare.

## References

- 1 A. Jaeger-Waldau, *PV Status Report 2019*, EUR 29938 EN, Publications Office of the European Union, Luxembourg, 2019, DOI: 10.2760/326629.
- 2 M. Taylor, P. Ralon, H. Anuta and S. Al-Zoghoul, *Renewable power, generation cost*, International Renewable Energy Agency, Abu Dhabi, 2020.
- 3 H. Idriss, Hydrogen production from water: past and present, *Curr. Opin. Chem. Eng.*, 2020, **29**, 74–82.
- 4 A. Ziani, I. Al-Shankiti, M. A. Khan and H. Idriss, Integrated Photo-Electrocatalytic (PEC) Systems for Water Splitting to Hydrogen and Oxygen under Concentrated Sunlight: Effect of Internal Parameters on Performance, *Energy Fuels*, 2020, **34**(10), 13179–13185.
- 5 M. Khan, I. Shankiti, A. Ziani, N. Wehbe and H. Idriss, A Stable Integrated Photoelectrochemical Reactor for  $\text{H}_2$  Production from Water Attains a Solar-to-Hydrogen Efficiency of 18% at 15 Suns and 13% at 207 Suns, *Angew. Chem.*, 2020, **59**, 14802–14808.
- 6 B. Parkinson, P. Balcombe, J. Speirs, A. Hawkes and K. Hellgardt, Levelized cost of  $\text{CO}_2$  mitigation from hydrogen production routes, *Energy Environ. Sci.*, 2019, **12**(1), 19–40.
- 7 M. R. Shaner, H. A. Atwater, N. S. Lewis and E. W. McFarland, A comparative technoeconomic analysis of renewable hydrogen production using solar energy, *Energy Environ. Sci.*, 2016, **9**(7), 2354–2371.
- 8 D. Yadav and R. Banerjee, Net energy and carbon footprint analysis of solar hydrogen production from the high-temperature electrolysis process, *Appl. Energy*, 2020, **262**, 114503.
- 9 J. Hinkley, J. Hayward, R. McNaughton, R. Gillespie, A. Matsumoto, M. Watt and K. Lovegrove, Cost assessment of hydrogen production from PV and electrolysis, *Report to ARENA as Part of Solar Fuels Roadmap, Project A-3018*, 2016, pp. 1–4.
- 10 S. Alsayegh, R. Varjian, Y. Alsalik, K. Katsiev, T. Isimjan and H. Idriss, Methanol Production Using Ultrahigh Concentrated Solar Cells: Hybrid Electrolysis and  $\text{CO}_2$  Capture, *ACS Energy Lett.*, 2020, **5**(2), 540–544.
- 11 IEA, *The Future of Hydrogen: Seizing Today's Opportunities*, 2019, <https://www.iea.org/reports/the-future-of-hydrogen>.
- 12 L. C. Andreani, A. Bozzola, P. Kowalczewski, M. Liscidini and L. Redorici, Silicon solar cells: toward the efficiency limits, *Adv. Phys.*, 2019, **4**(1), 1548305.
- 13 M. A. Green, E. D. Dunlop, D. H. Levi, J. Hohl-Ebinger, M. Yoshita and A. W. Y. Ho-Baillie, Solar cell efficiency tables (version 54), *Prog. Photovolt: Res. Appl.*, 2019, **27**(7), 565–575.
- 14 F. Dimroth, T. N. Tibbets, M. Niemeyer, F. Predan, P. Beutel, C. Karcher, E. Oliva, G. Siefer, D. Lackner and P. Fuß-



Kailuweit, Four-junction wafer-bonded concentrator solar cells, *IEEE Journal of Photovoltaics*, 2015, **6**(1), 343–349.

15 M. A. Green, E. D. Dunlop, D. H. Levi, J. Hohl-Ebinger, M. Yoshita and A. W. Ho-Baillie, Solar cell efficiency tables (version 54), *Prog. Photovoltaics*, 2019, **27**(7), 565–575.

16 M. Wiesenfarth, S. Philipps, A. Bett, K. Horowitz and S. Kurtz, Current status of concentrator photovoltaic (CPV) technology Version 1.3, *Fraunhofer Inst. Sol. Energy Syst. ISE*, Nat. Renewable Energy Lab., 2017.

17 M. Steiner, G. Siefer, T. Schmidt, M. Wiesenfarth, F. Dimroth and A. W. Bett, 43% sunlight to electricity conversion efficiency using CPV, *IEEE Journal of Photovoltaics*, 2016, **6**(4), 1020–1024.

18 M. Wiesenfarth, I. Anton and A. Bett, Challenges in the design of concentrator photovoltaic (CPV) modules to achieve highest efficiencies, *Appl. Phys. Rev.*, 2018, **5**(4), 041601.

19 W. J. Chang, K.-H. Lee, H. Ha, K. Jin, G. Kim, S.-T. Hwang, H.-m. Lee, S.-W. Ahn, W. Yoon and H. Seo, Design principle and loss engineering for photovoltaic–electrolysis cell system, *ACS Omega*, 2017, **2**(3), 1009–1018.

20 A. Nakamura, Y. Ota, K. Koike, Y. Hidaka, K. Nishioka, M. Sugiyama and K. Fujii, A 24.4% solar to hydrogen energy conversion efficiency by combining concentrator photovoltaic modules and electrochemical cells, *Appl. Phys. Express*, 2015, **8**(10), 107101.

21 J. Jia, L. C. Seitz, J. D. Benck, Y. Huo, Y. Chen, J. W. D. Ng, T. Bilir, J. S. Harris and T. F. Jaramillo, Solar water splitting by photovoltaic-electrolysis with a solar-to-hydrogen efficiency over 30%, *Nat. Commun.*, 2016, **7**(1), 1–6.

22 J. Proost, State-of-the art CAPEX data for water electrolyzers, and their impact on renewable hydrogen price settings, *Int. J. Hydrogen Energy*, 2019, **44**(9), 4406–4413.

23 W. G. Colella, B. James and J. M. Moton, *Hydrogen Pathways Analysis for Polymer Electrolyte Membrane (PEM) Electrolysis*, Strategic Analysis Inc, 2014.

24 S. Rehman, Solar radiation over Saudi Arabia and comparisons with empirical models, *Energy*, 1998, **23**(12), 1077–1082.

25 E. Zell, S. Gasim, S. Wilcox, S. Katamoura, T. Stoffel, H. Shibli, J. Engel-Cox and M. Al Subie, Assessment of solar radiation resources in Saudi Arabia, *Sol. Energy*, 2015, **119**, 422–438.

26 B. D. James, G. N. Baum, J. Perez and K. N. Baum, *Technoeconomic Analysis of Photoelectrochemical (PEC) Hydrogen Production*, DOE report, 2009.

27 V. D. Rumyantsev, V. M. Andreev, A. W. Bett, F. Dimroth, M. Hein, G. Lange, M. Z. Shvarts and O. V. Sulima, Progress in development of all-glass terrestrial concentrator modules based on composite Fresnel lenses and III-V solar cells, *Conference Record of the Twenty-Eighth IEEE Photovoltaic Specialists Conference*, Anchorage, AK, US, 2000, DOI: 10.1109/PVSC.2000.916096.

28 S. Restrepo-Valencia and A. Walter, Techno-Economic Assessment of Bio-Energy with Carbon Capture and Storage Systems in a Typical Sugarcane Mill in Brazil, *Energies*, 2019, **12**(6), 1129.

29 D. McIlveen-Wright, Y. Huang, S. Rezvani, J. D. Mondol, D. Redpath, M. Anderson, N. Hewitt and B. Williams, A techno-economic assessment of the reduction of carbon dioxide emissions through the use of biomass co-combustion, *Fuel*, 2011, **90**(1), 11–18.

30 M. Steinberg and H. C. Cheng, Modern and prospective technologies for hydrogen production from fossil fuels, *Int. J. Hydrogen Energy*, 1989, **14**(11), 797–820.

31 S. Ong, C. Campbell, P. Denholm, R. Margolis and G. Heath, *Land-use Requirements for Solar Power Plants in the United States*, National Renewable Energy Lab. (NREL), Golden, CO, United States, 2013.

32 K. Horowitz, M. Woodhouse, H. Lee and G. Smestad, *Bottom-Up Cost Analysis of a High Concentration PV Module*, National Renewable Energy Lab. (NREL), Golden, CO, United States, 2015.

33 X. Wang and A. Barnett, The evolving value of photovoltaic module efficiency, *Appl. Sci.*, 2019, **9**(6), 1227.

34 M. Bolinger, J. Seel and D. Robson, *Utility-Scale Solar: Empirical Trends in Project Technology, Cost, Performance, and PPA Pricing in the United States–2019 Edition*, 2019.

35 B. D. James, D. A. DeSantis and G. Saur, *Hydrogen Production Pathways Cost Analysis (2013–2016)*, Strategic Analysis Inc., Arlington, VA, United States, 2016.

36 Quoted by BSQ Solarin Madrid, S., <https://www.bsqsolar.com/>.

37 M. Bolinger and J. Seel, *Utility-scale Solar: Empirical Trends in Project Technology, Cost, Performance, and PPA Pricing in the United States*, LBNL, 2018.

38 M. Renzi, M. Santolini and G. Comodi, Performance analysis of a 3.5 kWp CPV system with two-axis tracker, *Energy Procedia*, 2014, **61**, 220–224.

39 R. Mikami, M. Inagaki, M. Moriguchi, K.-i. Kitayama, H. Konaka and T. Iwasaki, Advantages of Concentrator Photovoltaic System in High Solar Radiation Region, *SEI Tech. Rev.*, 2016, (82), 137.

40 S. Ponce-Alcántara, J. P. Connolly, G. Sánchez, J. M. Míguez, V. Hoffmann and R. Ordás, A statistical analysis of the temperature coefficients of industrial silicon solar cells, *Energy Procedia*, 2014, **55**, 578–588.

41 M. Khalis, R. Masrour, G. Khrypunov, M. Kirichenko, D. Kudiy and M. Zazoui, In Effects of temperature and concentration mono and polycrystalline silicon solar cells: extraction parameters, *J. Phys.: Conf. Ser.*, 2016, 012001.

42 D. C. Bobela, L. Gedvilas, M. Woodhouse, K. A. Horowitz and P. A. Basore, Economic competitiveness of III–V on silicon tandem one-sun photovoltaic solar modules in favorable future scenarios, *Prog. Photovoltaics*, 2017, **25**(1), 41–48.

43 J. E. Haysom, O. Jafarieh, H. Anis, K. Hinzer and D. Wright, Learning curve analysis of concentrated photovoltaic systems, *Prog. Photovoltaics*, 2015, **23**(11), 1678–1686.

44 D. Stolten and B. Emonts, *Hydrogen Science and Engineering, 2 Volume Set: Materials, Processes, Systems, and Technology*, John Wiley & Sons, 2016, vol. 1.

